Adhesion Promotion Mechanisms at Isotactic Polypropylene/Polyamide 6 Interfaces: Role of the Copolymer Architecture

Claire Laurens,[†,§] Costantino Creton,[‡] and Liliane Léger*[,†]

Laboratoire de Physique des Fluides Organisés, UMR CNRS-Collège de France 7125, 11 place Marcelin Berthelot, 75231 Paris Cedex 05, France, and Laboratoire de Physico-Chimie Structurale et Macromoléculaire, UMR CNRS-ESPCI 7615, 10 rue Vauquelin, 75231 Paris Cedex 05, France

Received January 30, 2004; Revised Manuscript Received June 16, 2004

ABSTRACT: The fracture toughness of isotactic polypropylene (iPP)−polyamide 6 (PA6) assemblies, stabilized by diblock copolymers formed in situ during the annealing of the samples, has been investigated as a function of annealing conditions and molecular architecture of the PP part of the copolymer. Comparing the evolutions of the fracture toughness with annealing time annealing temperature and surface density of copolymers for six different architectures, the reinforcement mechanisms could be qualitatively identified. It is thus possible to design an "optimal "copolymer for adhesion reinforcement: it has to have a molecular architecture as close as possible to that of the PP matrix and to be long enough so that it can bridge crystalline lamellae in the PP part of the sample, an effect which is favored when the annealing temperature is above the melting temperature of both parts of the assembly, due to an epitaxial orientation at the PP−PA6 interface.

Introduction

Most A/B polymer pairs are nonmiscible and present a mechanically weak interface due to the lack of entanglements between the two types of macromolecules. This prevents their use in polymer alloys, except if a compatibilizing component is added to avoid phase separation and prevent interfacial failure between the two phases. This additive can be a block copolymer (premade and blended or formed in-situ by a chemical reaction) that acts as a molecular connector entangled with bulk chains on both sides of the interface.[1−3] It decreases the interfacial tension between the two polymers and increases the mechanical strength of the interface by allowing stress transfer across the interface. We focus here on the mechanical role of the copolymer.

The molecular characteristics of the block copolymer required for an effective reinforcement of the interface between two glassy polymers are now relatively well-known.[4−6] For large enough molecular weights so that the diblock copolymer molecules can entangle with the two polymer matrices and for high enough surface density of copolymer, the stress that the interface can transfer becomes larger than the crazing stress of at least one of the two matrices. Plastic deformation occurs in the more ductile polymer, and an asymmetric craze propagates ahead of the crack tip. It is then possible to relate the fracture toughness of the interface G_c and the surface density of copolymer Σ through Brown's model for the toughness of glassy polymers[7] or its refinement by Sha et al.[8] The predictions of these models have been verified for several experimental systems.[7,9−11]

For semicrystalline polymers the situation is less clear, since the morphology and the crystallinity near the interface are likely to influence the plastic deformation mechanisms of the matrix as well as the coupling between the connecting chains and the matrix. A useful model system to investigate alloys between two semicrystalline polymers is the interface between isotactic polypropylene (iPP) and polyamide 6 (PA6): their adhesion properties have been particularly studied in the literature.[12−23] The interface is reinforced with iPP−PA6 copolymers formed in situ by chemical reaction between the $-NH_2$ end of polyamide chains and modified polypropylene chains bearing acid or anhydride groups. The copolymer is most usually a diblock copolymer obtained by the mean of a succinic anhydride functionalized polypropylene. These functionalized molecules, able to react with the amine end of the PA6 molecules, are mixed with the PP matrix, and the copolymer is formed during an annealing above the iPP melting temperature.[12−21] The use of hyperbranched polypropylenes[22,24,25] and the direct functionalization of the iPP matrix by a radiation beam have also been reported.[23]

Boucher et al.[12] have shown that the influence of connecting diblock copolymer chains on the fracture toughness of such assemblies is, in most experimental conditions, similar to what is observed for assemblies of glassy polymers. However, in some cases,[12,13] the measured fracture toughness was crucially dependent on details of the annealing conditions and on the molecular weight of the copolymer, in ways that could not be accounted for by the existing theories valid for glassy polymers. In particular, several interesting observations were made: (i) When the annealing temperature of the assembly was above the melting point of PA6 and for high enough molecular weights of the formed diblock, the measured G_c was 4 times larger than the equivalent sample annealed at lower temperature,[13] at given surface density of copolymer. (ii) The kinetics of formation of copolymer was rather slow and diffusion-controlled.[14] (iii) For each annealing temperature, the surface density of copolymer first increased

† UMR CNRS-Collège de France 7125.
‡ UMR CNRS-ESPCI 7615.
§ Present address: Cray Valley, Research Center of Oise, Parc Alata, B.P 22, 60550 Verneuil en Halatte, France.
* To whom correspondence should be addressed. E-mail Liliane.leger@college-de-france.fr.

10.1021/ma0400259 CCC: $27.50
Published on Web 08/07/2004

with annealing time and then saturated, at a value which depended on the annealing temperature.[13]

In subsequent studies, both the structure of the plastic zone formed ahead of the crack tip and the organization of the crystalline structure within the first microns near the interface were investigated by transmission electron microscopy. A correlation between high fracture toughness of the assembly and the existence of diffuse deformation zones further away from the interface[15−17] was put into evidence. This did not, however, shed light on the reason why these diffuse deformation zones could develop.

These observations led us to suspect that the specific nature of the coupling (entanglements, crystallization in the same lamella) in the immediate vicinity of the interface between the semicrystalline iPP matrix and the PP block of the PP−PA6 block copolymer could be a crucial point in determining adhesive strength.

To further investigate these issues we followed two paths: (1) We developed methods to characterize the crystallinity within the first 50 nm of the interface by grazing angle X-ray diffraction techniques on thin films assemblies. (2) We synthesized a series of succinic anhydride functionalized PP's with different molecular architectures (isotactic-PP, isotactic-PP with 5% PE, syndiotactic-PP, metallocene-PP) and investigated their potential use as interface modifiers in the same iPP matrix.

In a first study using grazing angle X-ray diffraction techniques on thin films,[18] interfaces between iPP and PA6 reinforced with the same block copolymers as those used in the Boucher et al. studies were investigated. These copolymers were based on a backbone chain of iPP containing 5% ethylene monomers. The key results were[18] the clear identification of an epitaxial crystallization of the iPP on the PA6 layer and evidences of a low miscibility of the succinic anhydride functionalized chains with the iPP matrix, leading to the formation of aggregates. At the interface, because of the epitaxy, the PP block of the copolymer chains was locally oriented parallel to the interface. The degree of epitaxial orientation was observed to vary with annealing time and temperature in ways quite similar to the fracture toughness.[18]

This observed correlation between adhesion and crystalline orientation in the immediate vicinity of the interface has been the starting point of the present systematic investigation on the role of crystallinity and molecular architecture of the block copolymer in iPP−PA6 interface reinforcement. In the present paper we focus on the role of the architecture of the PP block of the copolymers on its ability to transfer interfacial stress, keeping the structure of the PP matrix constant. The structure and miscibility of the products were first characterized. The fracture toughness of macroscopic samples and the areal density of copolymer formed at the interface were then measured to correlate the copolymer architecture and crystalline structure at the interface to the adhesion reinforcement at iPP/PA6 interfaces.

Experimental Section

Materials. The polyamide 6 was Ultramid B3 from BASF, having an average of one $-NH_2$ end per chain. Isotactic polypropylene 3050MN1 from Appryl/Atofina was used for the other part of the assemblies. The characteristics and main properties of the polymer matrix are listed in Table 1. The PP matrix was melt blended with 5 wt % of succinic anhydride functionalized polypropylenes (PP_f), having one average anhydride per chain. Such blends will be denoted iPP* in the following. The iPP* blends were available as extruded sheets with an approximate thickness of 500 μm. The PA6 was molded at 250 °C into plates with thickness between 0.8 and 2 mm. All polymer sheets were washed in an ultrasonic bath with ethanol and *n*-heptane before use. The PA6 sheets were dried at 80 °C under vacuum for 3 days and stored under vacuum in order to minimize the moisture sorption by PA6 and its effects on the PA6 mechanical properties.

Table 1. Molecular Characteristics and Properties of the Polymer Matrix

product	M_n (kg/mol)	M_w/M_n	E (GPa)[a]	σ_y (MPa)[b]	T_c (°C)[c]	T_m (°C)[d]	χ (%)[d]
PA6	18	1.9	2.9[e] to 1.0 [f]	65[f]	∼190	221	∼30
iPP	57	4.8	1.25	27	∼117	165.5	∼45

[a] Measured by three-points bending test. [b] Measured by traction tests. [c] Cooling rate: 5 °C/min. [d] Data recorded on the DSC second heating scan. [e] Dry PA6. [f] Wet PA6.

Five different PP_f were provided by Atofina. A first series was prepared by grafting PP 3050 MN4 from Appryl (an ethylene−propylene copolymer) with maleic anhydride by reactive extrusion. Two molecular weights were available, which will be called in the following "l-M_n PE-PP_f" and "h-M_n PE-PP_f" (for respectively the lower and the higher molecular weight PP_f). These products are those used in previous studies.[12,13,16,18] The second series was prepared by reaction in solution. A pure isotactic polypropylene obtained by Ziegler−Natta catalysis (PP 3050BN1 from Appryl/Atofina) and a pure isotactic polypropylene obtained by metallocene catalysis were successively grafted with maleic anhydride. The grafting of PP 3050 BN1 gave two PP_f with molecular weights similar to those obtained from the PP 3050 MN4 ethylene−propylene copolymer. They will be called "l-M_n iPP_f" and "h-M_n iPP_f" in the following. The product obtained from the metallocene iPP will be called "miPP_f". The main physical characteristics of these different PP_f are summarized in Table 2. Their molecular architecture was characterized by ^{13}C NMR. The measurements were carried out at 75 MHz in 1,2,4-trichlorobenzene at 120 °C (7 wt % solution) with deuterated tetrachloroethane as an external lock. The iPP matrix and PP_f proved to have almost the same tacticity with about 80% of meso pentads and less than 5% of racemic pentads. The exact molecular structures of the other PP's were very different. The backbone of the PE−PP_f appeared to be an ethylene−propylene block copolymer containing about 13.5% of short polyethylene blocks (∼3−4 monomers). The iPP_f and miPP_f are pure polypropylene chains, but the miPP_f spectra showed peaks characteristic of the presence of many regioirregularities (head-to-head and tail-to-tail links).

Solvents and chemical reactives were used as received. Formic acid (analysis grade, purity > 98%), dichloromethane (analysis grade, purity > 99.9%), and acetone (purity 99.5%) were purchased from SDS, trifluoroacetic anhydride was from Aldrich (purity > 99%), and xylene, *n*-heptane, and ethanol were from Prolabo ("Normapur" grades).

DSC Characterization. All the products were characterized by a modulated DSC on a T.A. Instruments 2820 apparatus. Heating and cooling rates were 5 °C/min, the modulation amplitude was 0.796 °C, and the modulation period was 60 s. The melting (crystallization) temperature was taken as the temperature at the maximum of the fusion (crystallization) peak. The crystalline fractions χ were calculated using the most current values for the heats of fusion of pure polymer crystals, that is, ΔH_m^0(PA6) = 230 J/g and ΔH_m^0(iPP) = 207 J/g.[26]

To characterize the ability of the PP_f to cocrystallize with the PP matrix, we also characterized PP* and 50/50 (w/w) matrix/PP_f blends by DSC. These blends were prepared by mixing the polymers in hot xylene under an argon atmosphere. The solutions were then precipitated in acetone. The precipitates were subsequently filtered, rinsed with acetone, and dried at 80 °C for at least 24 h before the DSC experiments.

Table 2. Molecular Characteristics and Properties of the Grafted Polypropylenes

PP_f	M_n (kg/mol)	M_w (kg/mol)	M_w/M_n	T_c (°C)[a]	T_m (°C)[b]	χ (%)[b]	architecture
l-M_n PE−PP_f	22.6	61	2.7	117	160	∼35	PP−PE copo with 13% PE
h-M_n PE−PP_f	43.0	141.9	3.3	116	163	∼39	PP−PE copo with 13%PE
l-M_n iPP_f	21.4	70.6	3.3	–[c]	–	–	pure PP, 80% meso pentads/5% racemic
h-M_n iPP_f	44.7	134.1	3.0	118	161	∼44	pure PP 80% meso pentads/5% racemic
miPP_f	69.7	216.1	3.1	109	140	∼32	pure PP with many regio -irregularities

[a] Cooling rate: 5 °C/min. [b] Data recorded on the DSC second heating scan. [c] A dash means that the measurement could not be made.

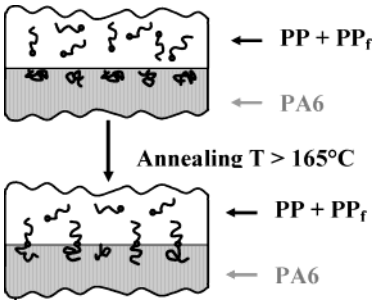

Figure 1. Schematic representation of an assembly: two sheets of PA6 and the blend of i$PP-PP_f$ are put into contact in a tight mold. Under annealing above the melting temperature of PP, the PP_f molecules can diffuse toward the interface and covalently bind to the NH_2 extremity of a PA6 molecule to form a diblock copolymer at the interface.

Fracture Toughness Measurements. The procedures for sample preparation, characterization of the fracture toughness (G_c), and characterization of the areal density of copolymer at the interface (Σ) are inspired by those developed by Boucher et al.[12,13] and are detailed in Laurens et al.[19] We just recall here what is necessary for the understanding of the present study.

G_c was measured using an asymmetric double-beam cantilever test (ADCB). A simple joint geometry was chosen for samples with fracture toughness below 170 J/m^2 ($h_{PA6} = 0.80-1.00$ mm and $h_{PP} = 1.40-2.00$ mm). For samples with $G_c >$ 170 J/m^2, a "sandwich" PA6/iPP/PA6 geometry with $h_{PA6} = 1.35-2.00$ mm and $h_{PP} = 0.50-0.75$ mm was used to avoid plastic deformation of the PP beam. This sandwich geometry was shown to be equivalent to the simple joint geometry for adhesion energies below 170 J/m^2.[13] The samples were annealed at temperatures between 185 and 223 °C to allow the formation of the copolymer as schematically presented in Figure 1. Equations 1 and 2, based on the "beam on an elastic foundation" model proposed by Kanninen[27] to take into account the finite elasticity of the materials ahead of the crack tip, were used to evaluate G_c.

$$G_c = \frac{3}{8}\frac{\Delta^2}{a^4}\frac{E_1 h_1^{\,3} E_2 h_2^{\,3}}{E_1 h_1^{\,3}\alpha_2^{\,2} + E_2 h_2^{\,3}\alpha_1^{\,2}} \quad (1)$$

with

$$\alpha_i = \frac{1 + 3/\lambda_i a + 3/(\lambda_i a)^2 + 3/2(\lambda_i a)^3}{1 + 1/\lambda_i a} \quad \text{and} \quad \lambda_i^{\,4} = \frac{6}{h_i^{\,4}} \quad (2)$$

E_i and h_i are respectively the Young's modulus and thickness of the beam i. For the sandwich geometry, the equivalent modulus of the composite PP/PA6 beam was calculated. Equation 1 gave consistent values of G_c as long as the ratio a/h_{PA6} was kept between 4 and 14 and for a ratio $h_{PP}/(h_{PP} + h_{PA6})$ in the range (0.57−0.70) for the simple joint geometry.[12] Taking into account the standard deviation on the measurement of a and the uncertainties on the physical constants and thickness of the beams, the estimated accuracy on G_c was about 10%.

Determination of the Copolymer Surface Density Σ. X-ray photoelectron spectroscopy (XPS) was used to determine Σ, after selective dissolution of the PA6 part of the assembly. For bulk samples (unbroken part of ADCB samples on which G_c had been measured), the method developed by Boucher et al.[12] was used, involving PA6 dissolution with three successive formic acid baths, followed by a treatment with trifluoroacetic anhydride in the gas phase and an hydroxylation in deionized water. We also determined Σ on iPP/PA6 thin films assemblies (total thickness about 110 nm), similar to the ones used to characterize the crystalline orientation at the interface[18,19] with a simplified protocol to dissolve the PA6 part (only two formic acid baths). In the first and most delicate step, the PP films were floated on the acid surface and picked up on clean macroscopic iPP films. The samples were then placed in a second acid bath for 1 h, dried under argon, rinsed with *n*-heptane and ethanol, and further dried. All the samples were stored in glass flasks cleaned with a "piranha" mixture and analyzed within 10 days of preparation to minimize the oxidation of the PA6 layer. The XPS spectra were subsequently collected on a SSX-100 Surface Science spectrometer using a monochromatic source (Al Kα_1, $h\nu = 1486.6$ eV). Survey scans between 0 and 1100 eV were first collected on each sample to check for surface contamination. The 1s spectra of carbon, nitrogen, and oxygen were then recorded on a clean area of the sample. Only the C 1s and N 1s signals were used to estimate Σ:[12]

$$\Sigma = -\frac{N_A \rho \lambda \sin\theta}{M_n} \ln\left(1 - \frac{I_N/I_C}{I_N^\infty/I_C^\infty}\right) \quad (3)$$

where N_A is Avogadro's number, ρ the mass density of PA6, M_n its number-average molar mass, λ the mean free path of N 1s photoelectrons, and θ the takeoff angle (35°). I_C, I_N, I_C^∞, and I_N^∞ are the respective intensities of the carbon and nitrogen peaks for the analyzed sample and pure PA6. The reproducibility of the Σ measurements was approximately ±10%.

Results

PP_f/Matrix Miscibility and Cocrystallization. Because of their different molecular architectures, the various PP_f were expected to have different degrees of miscibility with the iPP matrix. TEM observations of macroscopic samples[16] as well as optical microscopy observations on thin films[28] showed that all PE−PP_f have a tendency to form aggregates in the iPP matrix: they probably self-associate via their PE blocks. Such aggregates were not observed in thin films formed with blends of iPP matrix with iPP_f. Direct observations of the miPP_f/iPP blends could not be made, but the only difference between the two backbones being the proportion of regioirregularities, they were expected to be at least partially miscible.

The DSC experiments carried out on the pure products showed that the melting and crystallization temperatures of iPP_f, PE−PP_f, and iPP matrix were very close (see Tables 1 and 2). The presence of a slight melting peak at 110 °C in the PE−PP_f DSC scans was observed, corresponding to the melting of the PE blocks. The presence of ethylene parts also led to a lower crystallinity than in pure iPP or iPP_f. The behavior of

Table 3. DSC Results for PP_f/Matrix Blends

	50/50 blends			PP* (5/95) blends		
PP_f	T_c (°C)[a]	T_m (°C)[b]	χ^b (%)	T_c (°C)[a]	T_m (°C)[b]	χ^b (%)
l-M_n PE−PP_f	118	163	∼41	120	164	∼44
h-M_n PE−PP_f	118	165	∼41	123	165	∼46
l-M_n iPP_f	−[c]	−	−	125	165	∼46
h-M_n iPP_f	119	163	∼44	124	165	∼44
miPP_f	116	162	∼37	122	165	∼45

[a] Cooling rate: 5 °C/min. [b] Data recorded on the DSC second heating scan. [c] A dash means that the measurement could not be made.

the 50/50 blends of PE−PP_f and iPP_f with the iPP matrix was however very close to that of the matrix. We thus concluded that these products are able to cocrystallize with the matrix (Table 3) despite the presence of PE blocks in the PE−PP_f molecules. The pure miPP_f was found to have a crystalline fraction as well as crystallization and melting temperatures much lower than those of the iPP matrix: the regioirregularities of the backbone probably delay the crystallization and the crystallites formed are smaller and less perfect than in the Ziegler−Natta iPP. However, the DSC scan of a 50/50 miPP_f/iPP blend showed only one crystallization peak and one melting peak (Figure 2 and Table 3) with T_c and T_m between those of the pure products. This is indicative of a cocrystallization of both types of chains: since the two T_c are well distinct, one would have expected two crystallization peaks or at least a very broad one if the products did not cocrystallize. The melting peak of the blend, however, was slightly broadened compared to those of the pure products, indicating a lot of defects in the crystallites due to the presence of the miPP_f. This also induced a decrease of the crystalline fraction compared to the pure iPP matrix. Thus, the three types of PP_f were found able to cocrystallize with the iPP matrix, the perfection of the crystals and the final crystalline fraction depending on the precise microstructure of the PP_f chains. In addition, we tested the DSC behavior of more diluted blends. Experiments were carried out on iPP* blends, containing 5% of PP_f in PP matrix. The results, given in the second column of Table 3, show that a small quantity of PP_f can induce the crystallization of the iPP matrix, the crystallization temperatures of such blends being about 5 °C above the one of the iPP matrix.

Kinetics of Copolymer Formation and Adhesion Enhancement. The values of G_c and Σ were measured as a function of the annealing time for the different samples. Figure 3 shows the kinetics of copolymer formation in thick samples at 200 °C. It is clear that the iPP_f reacted much faster with PA6 than the other PP_f. The surface density of copolymer Σ saturated almost immediately at the same Σ_{max} for both iPP_f while it increased more slowly and did not reach a plateau for the other PP_f, less miscible with the iPP matrix. These results are consistent with the kinetics of copolymer formation observed in thin films for the h-M_n iPP_f and for the two PE-PP_f annealed at 200 °C, as reported in Figure 4. The rate of formation of the copolymers in these films was also found to strongly depend on the PP_f microstructure. For the PE−PP_f copolymers, the shorter copolymer reacted faster than the long one, while both copolymers did not saturate the interface. On the contrary, the iPP_f reacted much faster than both PE−PP_f, and saturation in Σ was reached. Similar

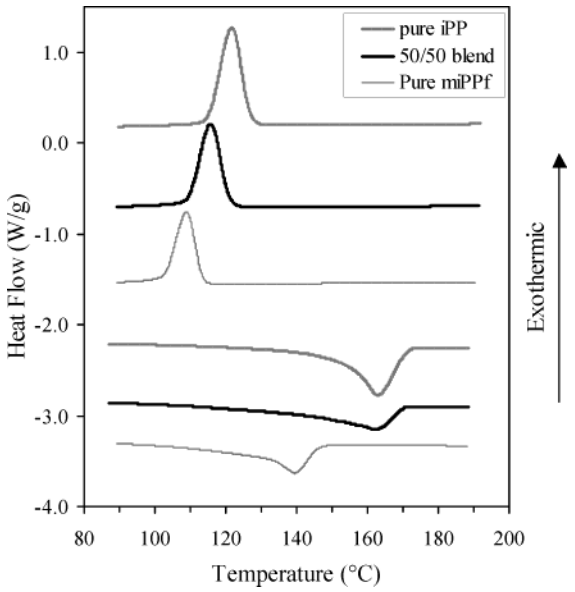

Figure 2. Crystallization and melting DSC scans of iPP, miPP_f, and a 50/50 iPP/miPP_f blend with a cooling (heating) rate of 5 °C/min.

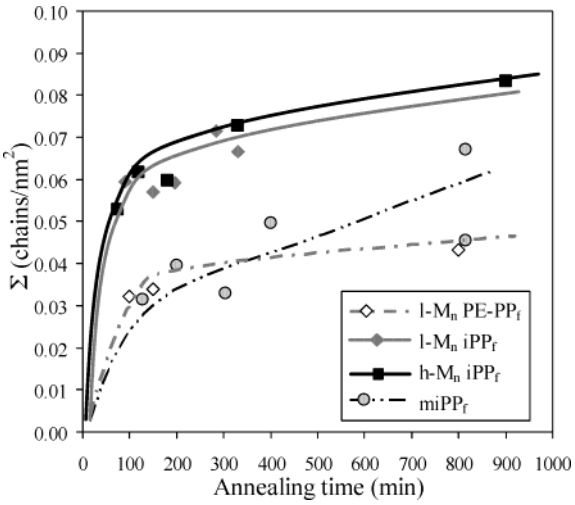

Figure 3. Influence of the PP_f structure on the copolymer formation kinetics in bulk samples. Samples annealed at 200 °C. The points corresponding to PE−PP_f are deduced from Boucher's results.[12] The lines are guides for the eyes.

results were obtained at higher annealing temperatures. Note that the maximum Σ obtained in thin films was lower than in bulk samples, indicating that the grafting of PP_f onto PA6 was limited by the total number of PP_f chains available in the thin film sample, while this was clearly not the case for the macroscopic samples.

As shown in Figure 5, the kinetics of adhesion enhancement at 200 °C was also strongly dependent on the molecular architectures of the PP_f. When the PP_f was fully compatible with the matrix (iPP/iPP_f filled symbols and plain lines), the adhesion energy increased rapidly and reached saturation with annealing time. When the PP_f was only partially compatible with the matrix (unfilled symbols and dotted lines), this increase was much slower and a plateau was not always observed. This is consistent with the Σ measurements which did not show a saturation of the interface by the copolymers at 200 °C for the corresponding PP_f. An important point is that the maximum G_c appeared to depend on the molecular weight of the PP block of the

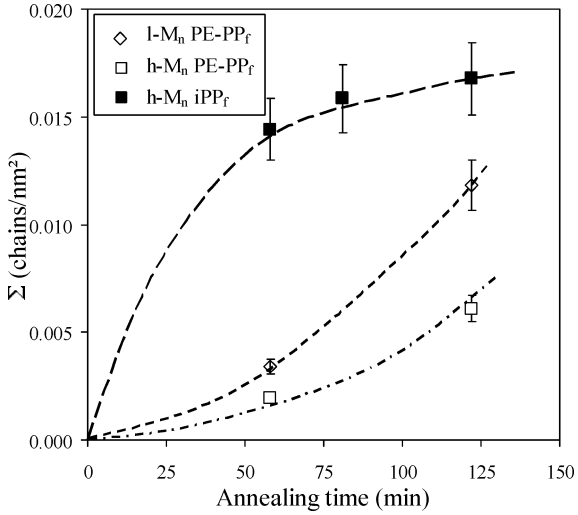

Figure 4. Influence of the PP_f structure on the kinetics of copolymer formation in thin films (thickness ~ 65 nm). The samples were annealed at 200 °C. The lines are guides for the eyes.

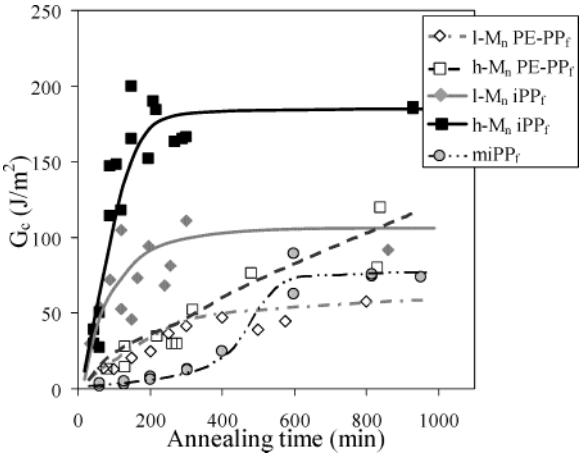

Figure 5. Influence of the PP_f and matrix structures on the kinetics of fracture toughness enhancement. Samples annealed at about 200 °C (except h-M_n PE-PP_f, annealed at 213 °C). The points corresponding to PE−PP_f are taken from Boucher's results.[12,13] The lines are guides for the eyes.

copolymer for both iPP_f and PE−PP_f ($G_{c,max}$ being larger for the high molecular weight PP_f) in opposition to the maximum Σ value in the case of the iPP_f, which was independent of the molecular weight.

The influence of annealing temperature and PP_f microstructure on the maximum G_c is shown in Figure 6. h-M_n iPP_f leads to the maximum fracture toughness whatever the annealing temperature. It is also clear from Figure 6 that annealing the samples above the PA6 melting temperature increased strongly the adhesion in samples containing h-M_n iPP_f and h-M_n PE-PP_f while such an increase was not observed in other cases. A sufficient molecular weight of the PP_f appears thus as a necessary condition to obtain a maximum toughness of the interface at high annealing temperatures, whatever the precise molecular structure of the PP_f.

Fracture Toughness G_c as a Function of the Surface Density of Copolymer Σ. To understand which mechanism is responsible for the interface reinforcement, it is useful to examine the relationship between G_c and Σ. In the case of glassy polymers it has been shown that a low G_c (a few J/m²) and a scaling $G_c \propto \Sigma$ are typical of a rupture mechanism by extraction

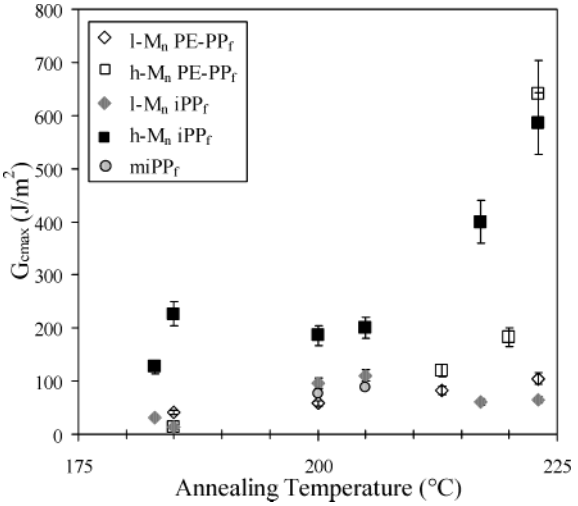

Figure 6. Influence of the annealing temperature on the maximum G_c obtained for the different types of samples (maximum annealing time ~ 900 min). The points corresponding to PE−PP_f are taken from Boucher's results.[12,13]

of the copolymer chains.[29] Higher values of G_c (10 J/m² to a few 100 J/m²) are on the contrary typical of a rupture by crazing and copolymer scission. The scaling is then given by $G_c \propto \Sigma^2$ (Brown's model[7]) or by the more refined model by Sha et al.,[8] giving $G_c \propto 1/\ln(1 - (\Sigma^*/\Sigma)^2)$. Considering Boucher et al.'s results,[12,13] a behavior in agreement with Brown's model was expected for all PP_f. The results reported in Figures 7−9 clearly show that all the samples did not follow such a behavior.

The data corresponding to the two high molecular weights PP_f are reported in Figure 7. The two systems have similar behaviors. For both types of samples the data recorded for annealing temperatures below the melting temperature of PA6 were consistent with a fracture mechanism through crazing and chain scission, as described by Brown[7] and Sha et al.[8] For higher annealing temperatures, a strong increase in fracture toughness compared to the predictions of the models is observed for both PP_f. In h-M_n PE−PP_f samples, this increase was related to the appearance of diffuse deformations zones in the PP beam, in addition to the main plastic zone[15,16] at the crack tip. We could not check the presence of such deformations by TEM in h-M_n iPP_f samples, but we observed that the PP side of the sample turned white in the vicinity of the interface, which is characteristic of significant deformations in the beam. The fact that h-M_n iPP_f samples exhibited the same behavior as h-M_n PE-PP_f implies that, for this molecular weight, the efficiency of iPP_f−PA6 and PE−PP_f−PA6 copolymers in transferring stress across the interface was equivalent for a given Σ, independently of the precise molecular architecture of the PP_f. Besides, the behavior of iPP_f−PA6 at high temperature confirmed the anomalous degree of reinforcement of high molecular weight copolymers first observed by Boucher et al.[13] The main difference between the two PP_f is then only a reaction rate with PA6 far greater for iPP_f than for PE−PP_f (Figures 3 and 4).

The $G_c(\Sigma)$ relationship was less clear for the other types of PP_f. The behavior of the low molecular weight PP_f is reported in Figure 8. As shown by Boucher et al.,[12] the l-M_n PE−PP_f had a reinforcing effect consistent with Brown's model, with a $G_c \propto \Sigma^2$ scaling. It is evident that the l-M_n iPP_f had a very different (and unexpected) behavior. For annealing temperatures above 190 °C, the

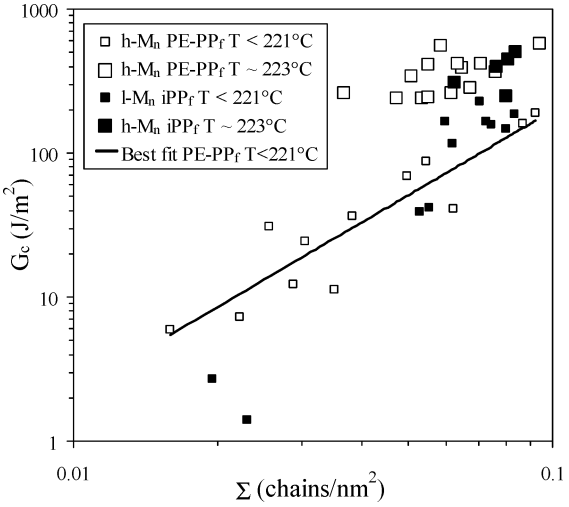

Figure 7. G_c as a function of Σ and temperature for the iPP/PA6 interface for high molecular weight PP_f. The best fit for data below 221 °C is also reported. This fit is consistent with Brown's model when using the values determined by TEM for the fibril diameter and extension and reasonable approximations for the unknown mechanical parameters of the PP craze.[16]

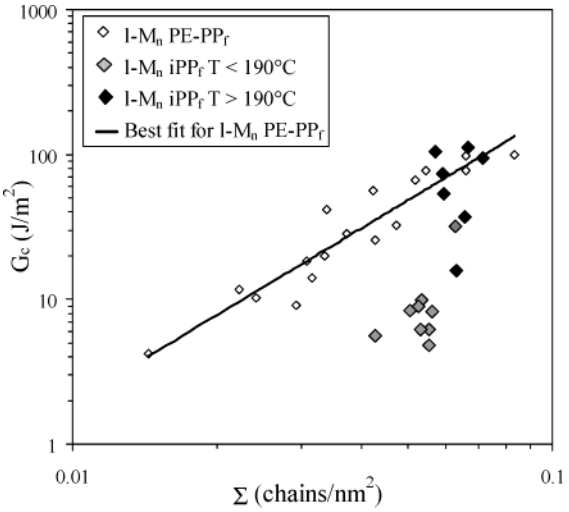

Figure 8. G_c as a function of Σ and temperature for the iPP/PA6 interface for low molecular weight PP_f. The best fit for l-M_n PE−PP_f data is also reported. This fit is consistent with Brown's model when using the values determined by TEM for the fibril diameter and extension and reasonable approximations for the unknown mechanical parameters of the PP craze.[16]

data for iPP_f were consistent with the behavior observed for l-M_n PE−PP_f. But for the lowest annealing temperatures, the adhesion energies were much lower (less than 10 J/m^2 except for the longest annealing time) while the interfacial copolymer densities were relatively high. The values of G_c were mostly in the range observed when fracture occurs by pullout of the copolymer from the matrix. These data seem to indicate a pullout to crazing transition for the l-M_n iPP_f-based copolymer, but this transition seems to depend mainly on the annealing temperature and not directly on the copolymer molecular weight. Figure 9 shows the data for the copolymers based on "metallocene" iPP_f: the behavior of most samples was in agreement a $G_c \propto \Sigma^2$ scaling, but some other samples presented a weaker adhesion. These weaker samples were those with the shortest annealing times (less than 200 min) and corresponded to the base

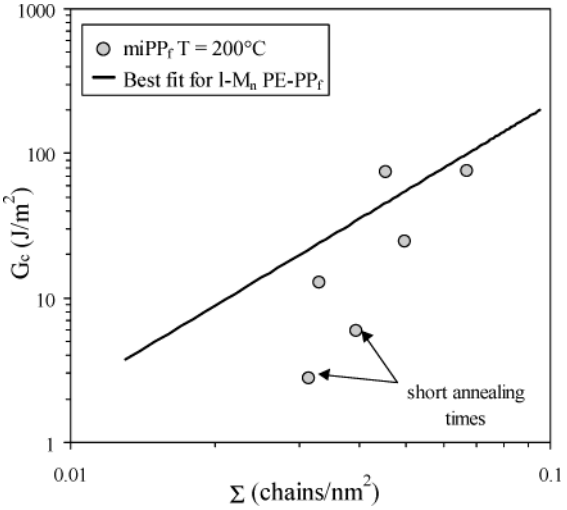

Figure 9. G_c as a function of Σ for the iPP/PA6 interface for metallocene iPP_f. The best fit for l-M_n PE−PP_f data is also reported as a reference.

of the S-shaped $G_c(t)$ curve observed for the miPP_f−PA6 copolymer (see Figure 5). All other samples were annealed at least 300 min, that is to say, after the first inflection of the $G_c(t)$ curve. This led us to think that Σ was not the only important parameter for the reinforcement of the PP/miPP_f−PA6/PA6 interface and that the annealing time should also be considered.

Discussion

Influence of the Copolymer Microstructure on the Kinetics. The kinetics of copolymer formation obtained for both thin films and macroscopic samples (Figures 3 and 4) as well as the kinetics of adhesion enhancement (Figure 5) show that the formation of the iPP_f−PA6 copolymers is much faster than the formation of the PE−PP_f−PA6 and miPP_f−PA6 copolymers. These kinetics thus appear directly linked to the PP_f molecular architecture, suggesting that the grafting of PP_f onto PA6 could be limited by the PP_f diffusion toward the interface for the PE−PP_f−PA6 and for the miPP_f−PA6.

The parameter limiting the rate of formation of the copolymers in such reactive systems is still a subject of discussion in the literature.[30−34] Theoretical works showed that the rate of formation of copolymer depends on the reactivity of the mutually reacting species, on their diffusion coefficient, and hence on the molecular weight of the polymer to which the reactive species is attached, and on the structure of the interface (area, roughness, etc.). Frederikson and Milner showed that the initial reaction rate is generally fast, but that the lack of reactive functions at the interface leads afterward to a regime controlled by the diffusion of the reactive species.[30,31] On the other hand, O'Shaughnessy et al.[32−34] showed that in the case of relatively low chemical reactivity (i.e., in all cases except when the reactive species are radicals) the reaction was not controlled by diffusion but by the species reaction rate, which depends on the temperature, the polymer molecular weight, and steric hindrance. Recent experimental studies[35,36] concluded that the formation of PS−PMMA and PS−PSMA copolymers, using amine-terminated PS, was limited by the reaction rate rather than by diffusion.In the iPP/PA6 system, we favored the hypothesis of a diffusion-limited reaction. Several experimental results are in favor of that hypothesis. Boucher et al.

suggested the existence of such a limitation in the l-M_n PE−PP_f case and estimated a diffusion coefficient for these molecules:[12] the obtained values, $D \cong 6 \times 10^{-12}$ cm^2/s at 185 °C and 16×10^{-12} cm^2/s at 213 °C, were consistent with established result on the diffusion of polyolefins in that range of temperatures. A recent work by Kim et al.,[23] on the adhesion of PA6 on iPP surfaces functionalized with carboxylic acids by irradiation, a system evidently not controlled by the diffusion of the reactive PP molecules, also showed a very fast copolymer formation: the interface was saturated by copolymers 30 min after the stabilization of the mold temperature, for annealing temperatures between 180 and 210 °C. The reaction rate between acid-functionalized iPP and PA6 is then very high. In the present study, the PP_f are anhydride-terminated. Anhydrides functions being more reactive than carboxylic acids, the reaction rates should be at least equal to those observed by Kim et al. If the copolymer formation was reaction-limited, we should observe a quick saturation of the interface by the copolymers, which is only the case for the iPP_f molecules. We thus conclude that the reaction between PP_f and PA6 is diffusion-limited for the PE−PP_f and for the $miPP_f$ but probably reaction limited in the iPP_f case. This is also consistent with the fact that the copolymer formation is slower for the "long" PE−PP_f chains than for the short ones.

This observed difference in the rate of copolymer formation can be rationalized owing to the differences in structure between PP_f and matrix. Indeed, in the PE−PP_f molecules, the presence of the ethylene blocks leads to an association of PE−PP_f molecules, as shown by optical microscopy observations of thin films.[16,28] A temperature-dependent equilibrium between free and associated chains can then affect the diffusion of the grafted molecules into the matrix and the copolymer formation. Along the same lines, the $miPP_f$ chains having a higher molecular weight than the matrix and bearing a lot of defects could also have difficulties to diffuse in the iPP matrix. In the iPP_f case, because of the close match between the molecular architectures of PP_f and iPP matrix the diffusion is rapid, and the reaction is probably not controlled by the diffusion of the grafted chains toward the interface: the observed reaction times are much shorter and the maximum Σ value depends neither on the annealing temperature nor on the molecular weight of the PP_f.

Influence of the Copolymer Molecular Architecture on the Interface Reinforcement. The set of results presented above shows that the molecular architecture of the copolymer strongly influences the iPP/PA6 interface reinforcement. All investigated systems cannot be described by a unique pattern, and the models used to describe the rupture of assemblies between glassy polymers are not sufficient to describe all the observed behaviors. Two main cases can be distinguished. When the iPP/PA6 interface is reinforced with l-M_n PE−PP_f-based copolymers, the measured fracture toughness is well described by Brown's and Sha' models. The results obtained on iPP/PA6 samples containing h-M_n PE−PP_f and h-M_n PE−PP_f are also in reasonable agreement with these models if the annealing temperature is below the melting temperature of PA6. In all other cases, the results deviate from the models, and the couple (G_c, Σ) is not sufficient to characterize the observed behaviors: one must consider other parameters such as annealing time and temperature.

In the absence of additional experiments such as direct observations of the deformed zones at the crack tip, we can only speculate on the possible reasons of such a discrepancy between results and models.

For samples containing $miPP_f$, the results are too preliminary to be discussed at length. It can just be noticed that the kinetics of copolymer formation are slow and that, on the basis of Figure 9, the grafted $miPP_f$ chains seem mechanically less effective than their iPP counterparts, a fact which could suggest a different stress transfer mechanism.

In the case of l-M_n iPP_f, the annealing temperature appears to be the additional parameter to consider: at low annealing temperatures, the measured adhesion was lower than expected whereas high annealing temperatures led to an enhanced efficiency of the copolymers. A possible explanation is not easy to find. As sufficiently long PP blocks are needed for efficiency, one would have to imagine that the molecular weight of the PP blocks of the copolymer is affected by the annealing temperature. The polydispersity of the copolymers is much larger than in previous studies on glassy polymers, and if the reaction at the interface is diffusion-limited, the relative amount of short and long PP_f molecules should depend on the annealing time, shorter chains being able to diffuse toward the interface faster than long one. It would then be possible that a very slight increase in Σ (i.e., in the annealing time for a given temperature) allows a few long chains to graft. It is then possible that the density of "long" chains grafted at the interface becomes sufficient to activate the crazing mechanisms. The fact that the transition between extraction and crazing takes place in a narrow range of molecular weights supports this hypothesis: chains having a backbone similar to the PE−PP_f, with $M_n \sim 16\,500$ g/mol and $M_w/M_n = 2.1$ having been proved to be extracted from the matrix,[15] contrary to l-M_n iPP_f. A slightly higher M_n and lower polydispersity for l-M_n PE-PP_f than for l-M_n iPP_f could explain that the extraction to crazing transition is not observed for l-M_n PE−PP_f. Nevertheless, in the absence of any way of characterizing the size of the grafted PP_f, it appears quite difficult to further verify this interpretation, unless being able to design systematic experiments with low-polydispersity samples.

In samples containing h-M_n PP_f, enhanced mechanical efficiency of the copolymers was observed when the annealing temperature was above the PA6 melting temperature, annealing conditions that also led to an enhanced degree of orientation of the polypropylene near the interface[18] Let us first examine the role played by the length of the copolymer chains in the reinforcement of polymer interfaces. In glassy assemblies, an optimum copolymer length exists at about $4-5M_e$:[4−6] the chains need to be sufficiently long to entangle with the matrix but not too long so that a sufficient Σ could be achieved. In semicrystalline polymers, the key parameter is probably not M_e but the mass necessary to achieve interlamellar links. Kramer's group recently studied the interface between syndiotactic polystyrene and polyethylene, a glassy (sPS)/semicrystalline (PE) interface.[37,38] Varying the molecular weights of the PE block, all above M_e, the reinforcement of the interface was observed to be optimum when the average radius of gyration of the PE block was greater than or equal

to the typical distance between two PE lamellae. The copolymer was then able to link several lamellae and transfer the stress at greater distances, leading to a better reinforcement of the interface than for shorter copolymer molecules.

For the present iPP/PA6 assemblies, all copolymers have a PP block with M_n greater than $3M_e$ (about 7 kg/mol for iPP): M_e is thus probably not the key parameter to consider. In iPP, the critical length for efficient connections between lamellae in the bulk has recently been estimated to be $M_w = M'_c \approx 200$ kg/mol.[39] This is greater than the M_w of all PP_f used here (about 135−140 kg/mol for the "long" ones and 60−70 kg/mol for the "short" ones). If the structure of the interface was equivalent to that of the bulk, none of the PP_f would be long enough to participate into interlamellar junctions. However, the interface has a particular crystalline structure due to the iPP/PA6 epitaxial relationship: in the zone in which epitaxy takes place, the number of PP chains locally oriented parallel to the interface is increased compared to bulk. As these chains participate into lamellae, one can assume that this increased orientation corresponds to an increased number of oriented lamellae. If the number of oriented lamellae close to the interface becomes larger, their mutual distance becomes smaller than in the bulk, and shorter chains could be able to bridge several lamellae. It would then be possible for the h-M_n PP_f to link several lamellae. The copolymer should then be able to transfer stress at larger distances. Such hypothesis is supported by several experimental observations. Indeed, annealing conditions leading to an important increase of epitaxial orientation (annealing temperatures greater than the PA6 melting temperature,[18,19] high cooling rate[19]) lead to an important increase of adhesion energy (ref 13 and the present study). The apparition of diffuse deformation zones in samples containing "long" PP_f chains and annealed above 221 °C could then be linked to an increase of the number of copolymer chains bridging several lamellae and able to transfer the stress at longer distances. On the contrary, copolymers with "short" iPP block should not be able to link several lamellae even if they are more closely packed than in the bulk due to epitaxy. Indeed, no reinforcement of the copolymer efficiency at 221 °C is observed for this type of copolymers. This would also explain why the short PP_f chains are less efficient than the long ones even at low temperatures (see Figures 4 and 5: at 200 °C, $G_{c,max}$ is 100 J/m^2 for l-M_n iPP_f and 200 J/m^2 for h-M_n iPP_f). In samples containing h-M_n PP_f some copolymer chains should be able to link two lamellae even at low annealing temperatures, whereas this linking would be impossible for the shorter chains.

At the present stage of the experiments, this explanation, even if plausible, remains qualitative because we have no way of characterizing the distance between lamellae in the immediate vicinity of the interface. (TEM observations may lead to direct observation of the lamellae, but the necessary staining, which concentrates at the interface, makes impossible to directly observe the microstructure within a few 10 nm from the interface.) A way to better validate the above hypothesis would be to use functionalized polypropylene chains with a higher molecular weight (with $M_w = M'_c$), able to link several lamellae even in the bulk in the iPP matrix, far from the epitaxial zone. If the above hypothesis is correct, such chains should be able to induce very high adhesion energies even at annealing temperatures below 221 °C.

Conclusion

The experiments presented above show that the adhesion at the PP/PA6 interface is governed by several parameters such as the molecular architecture and molecular weight of the products, the annealing conditions, the interfacial density of copolymer, and the crystalline structure at the interface. None of these parameters, alone, can account for all the observed phenomena, and coupling between these parameters needs to be considered.

The main results obtained can be summarized as follows. The more similar the molecular architectures of the copolymer and the PP matrix are, the faster is the rates of copolymer formation and of fracture toughness enhancement. The way in which the molecular structure influences the molecular mechanisms of interface reinforcement is less obvious. Brown's model, which accounts very well for the behavior at glassy interfaces, is not systematically followed by PP/PA6 interfaces, and the interfacial density of copolymer Σ is not the only important parameter for the reinforcement of these interfaces. The PP_f molecular weight, the annealing time, and temperature should also be considered. For instance, "long" copolymer chains appeared to be more efficient than the "short" ones to reinforce the interface, an effect that we relate to the ability of these chains to link several lamellae in the very vicinity of the interface thanks to the epitaxial orientation at the interface that brings the lamellae closer to one another. These interlamellar links probably allow the stress to be transferred at longer distances and could account for the higher adhesion as well as for the extended deformation observed in these samples.

This study also can be used as a guide to the design of an optimum PP_f for enhanced adhesion. It should have a molecular architecture as similar as possible to that of the matrix to give a rapid reaction at the PP−PA6 interface (the contact times in industrial processes being much shorter than those used in the present study). It should also have a high molecular weight so that it could bridge different lamellae and thus transfer the stress far from the interface. The question of the optimum in length is still open, too long chains leading to a reduction of Σ in reasonable contact times. We can also deduce from this study that optimum process conditions for a high adhesion at the PP/PA6 interface would probably be those leading to the development of the maximum epitaxy at the interface. This implies an annealing temperature above the melting temperature of both PP and PA6 and a fast cooling rate, both conditions that are usually achieved in industrial processes.

Acknowledgment. The authors thank Atofina for its financial support and for providing all the materials used in this study. We particularly thank Christian Quet (Atofina, Groupe de Recherches de Lacq) for access to the XPS apparatus and for his help in collecting the data. The ^{13}C NMR measurements were performed by Françoise Lauprêtre and Christine Sulpice-Gaillet from the Laboratoire de Recherche sur les Polymères (LRP, Thiais, UMR CNRS 7581).

References and Notes

(1) Fayt, R.; Jérôme, R.; Teyssié, P. *J. Polym. Sci., Part B: Polym. Phys.* **1989**, *27*, 775−793.

(2) Brown, H. R.; Deline, V. R.; Green, P. F. *Nature (London)* **1989**, *341*, 221−222.
(3) Creton, C.; Kramer, E. J.; Hadziioannou, G. *Macromolecules* **1991**, *24*, 1846−1853.
(4) Kramer, E. J.; Norton, L. J.; Dai, C.-A.; Sha, Y.; Hui, C. Y. *Faraday Discuss.* **1994**, *98*.
(5) Creton, C. In *Polymer Surfaces and Interfaces III*; Richards, R. W., Pearce, S. K., Eds.; John Wiley & Son Ltd.: New York, 1999; pp 101−147.
(6) Creton, C.; Kramer, E. J.; Brown, H. R.; Hui, C. Y. *Adv. Polym. Sci.* **2002**, *156*, 53−136.
(7) Brown, H. R. *Macromolecules* **1991**, *24*, 2752−2756.
(8) Sha, Y.; Hui, C. Y.; Ruina, A.; Kramer, E. J. *Macromolecules* **1995**, *28*, 2450−2459.
(9) Creton, C.; Kramer, E. J.; Hui, C. Y.; Brown, H. R. *Macromolecules* **1992**, *25*, 3075−3088.
(10) Char, K.; Brown, H. R.; Deline, V. R. *Macromolecules* **1993**, *26*, 4164−4171.
(11) Creton, C.; Brown, H. R.; Shull, K. R. *Macromolecules* **1994**, *27*, 3174−3183.
(12) Boucher, E.; Folkers, J. P.; Hervet, H.; Léger, L.; Creton, C. *Macromolecules* **1996**, *29*, 774−782.
(13) Boucher, E.; Folkers, J. P.; Creton, C.; Hervet, H.; Léger, L. *Macromolecules* **1997**, *30*, 2102−2109.
(14) Boucher, E. PhD Thesis, Université Paris VI-Pierre et Marie Curie, 1995.
(15) Kalb, F. PhD Thesis, Université Paris VI-Pierre et Marie Curie, 1998.
(16) Plummer, C. J. G.; Kausch, H.-H.; Creton, C.; Kalb, F.; Léger, L. *Macromolecules* **1998**, *31*, 6164−6176.
(17) Kalb, F.; Léger, L.; Creton, C.; Plummer, C. J. G.; Marcus, P.; Magalhaes, A. *Macromolecules* **2001**, *34*, 2702−2709.
(18) Laurens, C.; Ober, R.; Creton, C.; Léger, L. *Macromolecules* **2001**, *34*, 2932−2936.
(19) Laurens, C.; Ober, R.; Creton, C.; Léger, L. *Macromolecules*, in press.
(20) Bidaux, J.-E.; Smith, G. D.; Bernet, N.; Manson, J.-A. E.; Hilborn, J. *Polymer* **1996**, *37*, 1129−1136.
(21) Bidaux, J.-E.; Smith, G. D.; Manson, J.-A. E.; Plummer, C. J. G.; Hilborn, J. *Polymer* **1998**, *39*, 5939−5948.
(22) Jannerfeldt, G.; Boogh, L.; Manson, J.-A. E. *Polymer* **2000**, *41*, 7627−7634.
(23) Kim, H.-J.; Lee, K.-J.; Seo, Y. *Macromolecules* **2002**, *35*, 1267−1275.
(24) Jannerfeldt, G.; Boogh, L.; Manson, J.-A. E. *J. Polym. Sci., Part B: Polym. Phys.* **1999**, *37*, 2069−2077.
(25) Jannerfeldt, G.; Boogh, L.; Manson, J.-A. E. *Polym. Eng. Sci.* **2001**, *41*, 293−300.
(26) *Polymer Handbook;* John Wiley & Sons: New York, 1975.
(27) Kanninen, M. F. *Int. J. Fract.* **1973**, *9*, 83−91.
(28) Laurens, C. PhD Thesis, Paris VI-Pierre et Marie Curie, 2002.
(29) Xu, D. B.; Hui, C. Y.; Kramer, E. J.; Creton, C. *Mech. Mater.* **1991**, *11*, 257−268.
(30) Fredrickson, G. H.; Milner, S. T. *Macromolecules* **1996**, *29*, 1786−7390.
(31) Fredrickson, G. H. *Phys. Rev. Lett.* **1996**, *76*, 3440−3443.
(32) O'Shaughnessy, B.; Sawhney, U. *Phys. Rev. Lett.* **1996**, *76*, 3444−3447.
(33) O'Shaughnessy, B.; Vavylonis, D. *Europhys. Lett.* **1999**, *45*, 638−644.
(34) O'Shaughnessy, B.; Vavylonis, D. *Macromolecules* **1999**, *32*, 1785−1796.
(35) Jiao, J.; Kramer, E. J.; De Vos, S.; Möller, M.; Koning, C. *Macromolecules* **1999**, *32*, 6261−6269.
(36) Schulze, J. S.; Cernohous, J. J.; Akira, H.; Lodge, T. P.; Macosko, C. W. *Macromolecules* **2000**, *33*, 1191−1198.
(37) Benkoski, J. J.; Bates, F. S.; Kramer, E. J. *Proceedings of ACS Meeting,* Orlando, 2002.
(38) Benkoski, J. J.; Florese, P.; Kramer, E. J. *Macromolecules* **2003**, *36*, 3289−3302.
(39) Fayolle, B. PhD Thesis, E.N.S.A.M., 2001.

MA0400259